Modeling ECCD stabilization of resistive tearing modes

Thomas G. Jenkins, University of Wisconsin-Madison

in collaboration with

Dalton Schnack, Carl Sovinec, Chris Hegna, Jim Callen, Fatima Ebrahimi
University of Wisconsin-Madison

Scott Kruger, Johan Carlsson
Tech-X Corporation

Eric Held, Jeong-Young Ji
Utah State University

Bob Harvey, Alexander Smirnov
CompX

The SWIM project team
http://cswim.org

2 May 2009

CEMM meeting
Denver, CO

Goal of SWIM Slow MHD campaign – numerically simulate ECCD stabilization of neoclassical tearing modes

•Experimental efforts to stabilize neoclassical tearing modes (NTMs) via electron cyclotron current drive (ECCD) have been very successful [see review by La Haye, Phys. Plasmas **13**, 055501 (2006)]. Want to develop a self-consistent numerical model for simulating this physics.

•Relative smallness of ECCD-induced current (of same order as electric field) implies that the fluid moment expansion of MHD – with appropriate modifications – should adequately capture the relevant physics.

•Time-averaging over the rapid variation in RF fields, and making a quasilinear approximation, puts the kinetic equation in the form:

$$\frac{\partial f_\alpha}{\partial t} + \mathbf{v}\cdot\nabla f_\alpha + \frac{q_\alpha}{m_\alpha}(\mathbf{E}+\mathbf{v}\times\mathbf{B})\cdot\frac{\partial f_\alpha}{\partial \mathbf{v}} = C(f_\alpha) + Q(f_\alpha)$$

Gyrophase-averaged Fokker-Planck Coulomb collision operator

$$Q(f_\alpha) \equiv \frac{\partial}{\partial \mathbf{v}}\cdot\mathcal{D}\cdot\frac{\partial}{\partial \mathbf{v}}$$

Quasilinear diffusion tensor from RF source

RF effects appear in fluid equations for the individual species

- Taking fluid moments in the conventional manner yields

$$\frac{\partial n_\alpha}{\partial t} + \nabla \cdot (n_\alpha \mathbf{v}_\alpha) = 0 \qquad \text{(RF produces no particles)}$$

$$m_\alpha n_\alpha \left(\frac{\partial \mathbf{v}_\alpha}{\partial t} + (\mathbf{v}_\alpha \cdot \nabla)\mathbf{v}_\alpha \right) = n_\alpha q_\alpha (\mathbf{E} + \mathbf{v}_\alpha \times \mathbf{B}) - \nabla p_\alpha - \nabla \cdot \pi_\alpha + \mathbf{R}_\alpha + \mathbf{F}^{rf}_{\alpha 0}$$

$$\mathbf{F}^{rf}_{\alpha 0} \equiv \int m_\alpha \mathbf{v} Q(f_\alpha) d\mathbf{v} \qquad \text{(additional momentum imparted by RF waves)}$$

$$\frac{3}{2} n_\alpha \left(\frac{\partial T_\alpha}{\partial t} + (\mathbf{v}_\alpha \cdot \nabla) T_\alpha \right) + n_\alpha T_\alpha \nabla \cdot \mathbf{v}_\alpha = -\nabla \cdot \mathbf{q}_\alpha - \pi_\alpha : \nabla \mathbf{v}_\alpha + Q_\alpha + S^{rf}_{\alpha 0}$$

$$S^{rf}_{\alpha 0} \equiv \int \frac{1}{2} m_\alpha v^2 Q(f_\alpha) d\mathbf{v} \qquad \text{(additional energy imparted by RF waves)}$$

Can approximate f_α as a local Maxwellian here – RF perturbations are small

- Closure calculations for $\mathbf{q}_\alpha$ and π_α are also affected by RF.

In single-fluid MHD model, dominant ECCD effect is in Ohm's Law

$$\nabla \cdot \mathbf{B} = 0 \qquad \nabla \times \mathbf{B} = \mu_0 \mathbf{J}$$

$$\nabla \times \mathbf{E} = -\frac{\partial \mathbf{B}}{\partial t} \qquad \frac{\partial \rho}{\partial t} + \nabla \cdot (\rho \mathbf{u}) = 0$$

$$\rho \frac{\partial \mathbf{u}}{\partial t} + \rho(\mathbf{u} \cdot \nabla)\mathbf{u} = -\nabla p + \mathbf{J} \times \mathbf{B} - \nabla \cdot \mathbf{\Pi} + \sum_{\alpha} \mathbf{F}^{rf}_{\alpha 0}$$

ECCD contributes little momentum relative to ion momentum

$$\frac{3}{2} n \left(\frac{\partial T}{\partial t} + (\mathbf{u} \cdot \nabla) T \right) + p \nabla \cdot \mathbf{u} = -\nabla \cdot \mathbf{q} - \mathbf{\Pi} : \nabla \mathbf{u} + Q + \sum_{\alpha} S^{rf}_{\alpha 0}$$

Minimal heating of MHD fluid by ECCD

$$\mathbf{E} + \mathbf{u} \times \mathbf{B} = \eta \mathbf{J} + \frac{\mathbf{F}^{rf}_{e0}}{n |q_e|}$$

MHD Ohm's law has an extra term which competes with the electric field – nonnegligible. Effectively, a localized electromotive force.

Neglect effect of ECCD on closures for q and Π, for the moment

Physics of the ECCD/MHD interaction is present in resistive tearing mode growth

•The Rutherford equation describes magnetic island growth in toroidal fusion devices

bootstrap current destabilization

polarization current stabilization

ECRH effects

$$\frac{dw}{dt} = \frac{\rho_s^2}{\tau_R}[\Delta' + \Delta'_{bs} + \Delta'_{curv} + \Delta'_{pol} + \Delta'_{ECCD} + \Delta'_H]$$

matching index for resistive tearing modes

curvature stabilization

ECCD effects

•Both ECCD and neoclassical effects enter additively – balancing Δ' and Δ'_{ECCD}, we don't need to model full neoclassical physics. Easier simulations.

•Initially, stipulate the form of the extra term in Ohm's law (later, use RF codes):

$$\frac{\mathbf{F}_{e0}^{rf}}{n|q_e|} = -\frac{\eta\lambda\mathbf{B}}{\mu_0} f(\mathbf{x})g(t)$$

This ECCD/MHD model has been implemented in NIMROD

•Model localized deposition in NIMROD and its effect on resistive tearing modes, using a DIII-D-like equilibrium. Mesh packing used on (2,1) and (3,1) rational surfaces.

•Here, f(**x**) is a narrow Gaussian in the poloidal plan, centered on the (2,1) rational surface. It extends over 1/10 of the torus.

•The parallel current profile

$$\mu = \mu_0 \frac{\mathbf{J} \cdot \mathbf{B}}{B^2}$$

is initially toroidally symmetric, but is modified by the ECCD deposition.

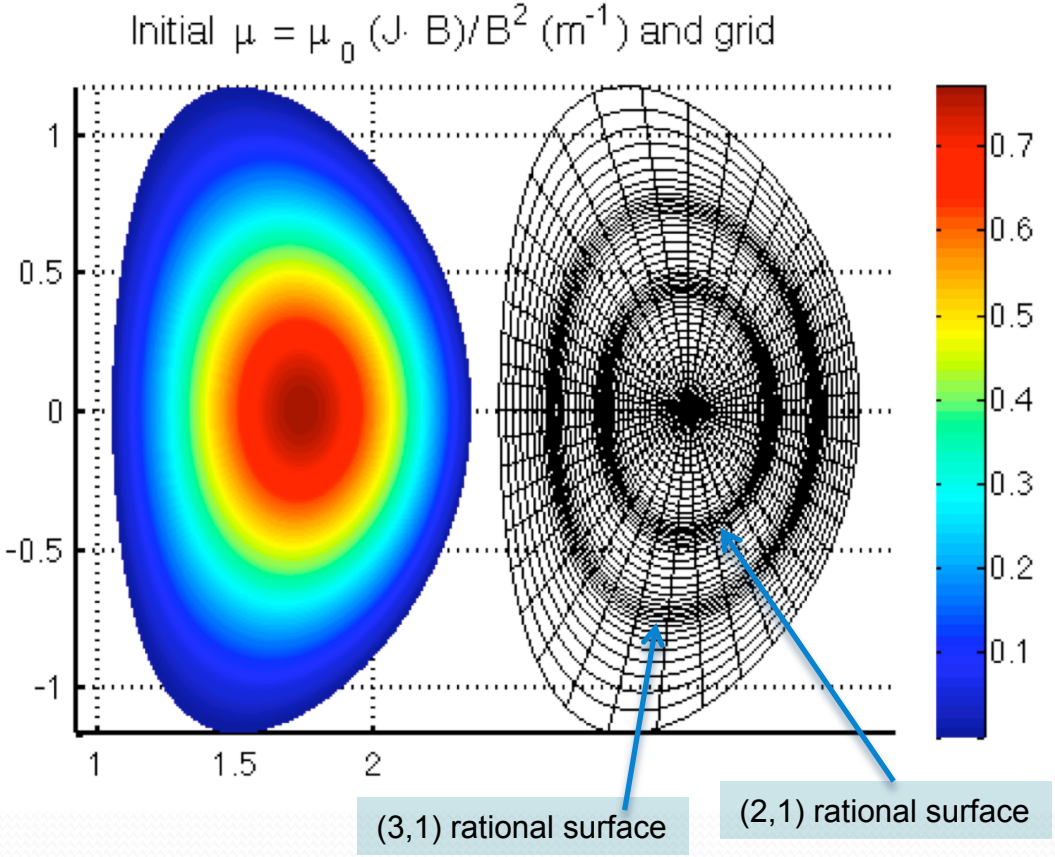

Localized ECCD deposition drives helical current filaments on rational surfaces

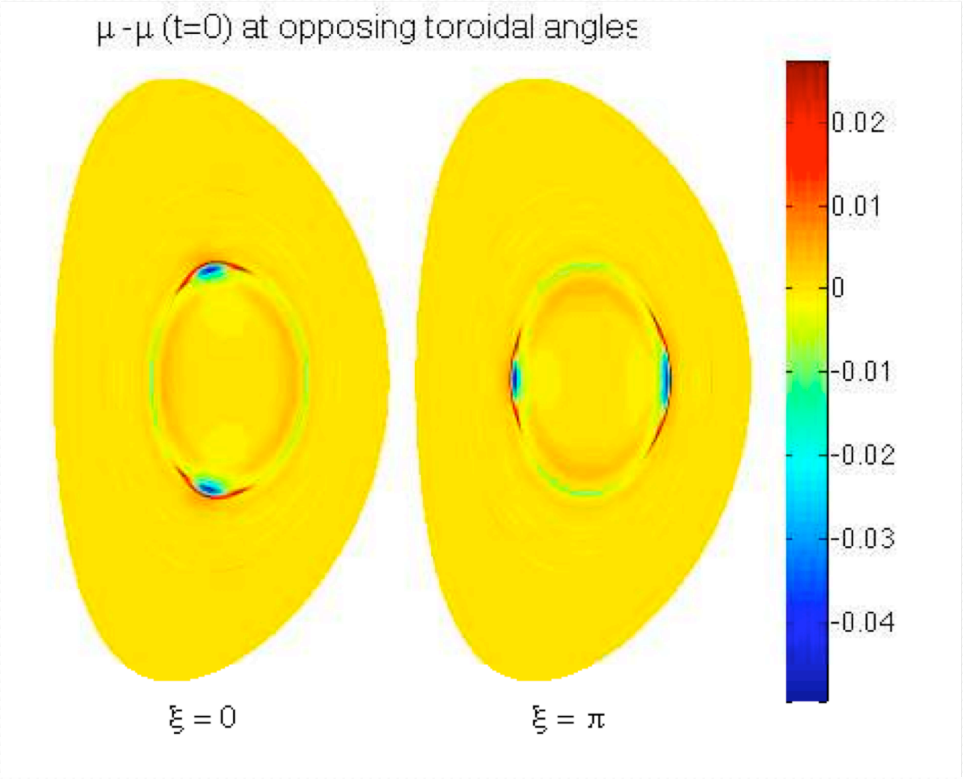

- At short times, ECCD launches Alfvén waves along the field lines it intercepts; at long times, it drives current along these field lines.

- On rational surfaces, field lines close and the perturbations have a helical structure. Nonlinear interactions occur, but are confined to the helical path.

ECCD-induced waves and currents are more complicated on nonrational surfaces

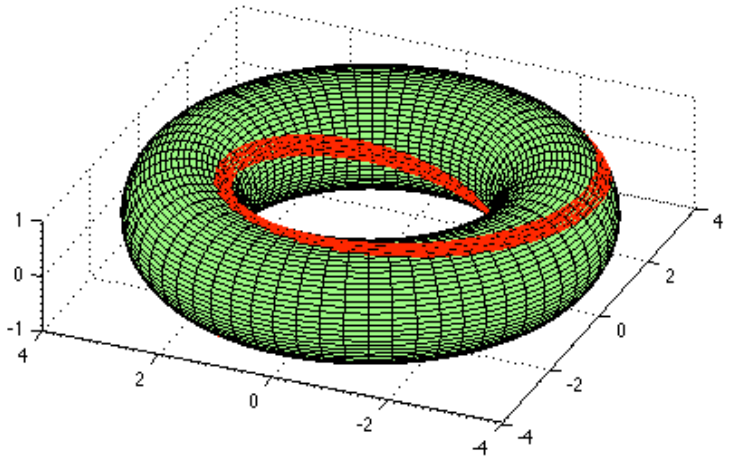

•The relevant physics on a rational surface (Alfvén waves and induced currents) occurs on a helical ribbon of field lines encircling the torus. Here q=2.

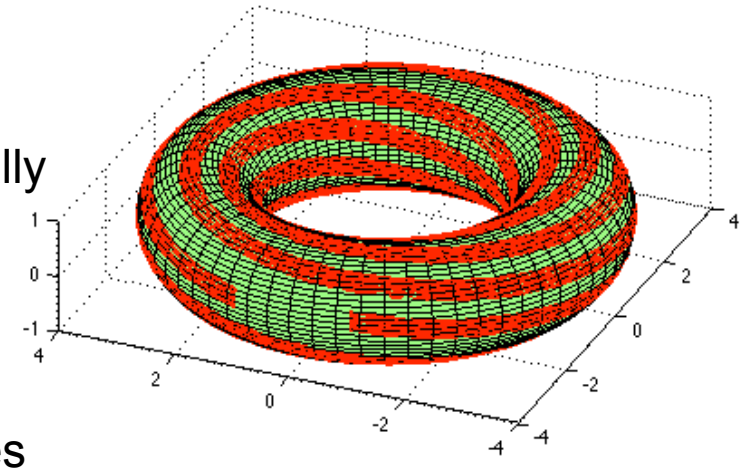

•On nonrational surfaces, the induced waves and currents (tied to field lines) must eventually cover the flux surface, just as the field lines do. Here q=2.23. Timescale for nonlinear wave-wave interactions may be much longer.

•To compare rational and nonrational surfaces on equal grounds (and see how well our model works), use toroidally symmetric ECCD deposition.

Without ECCD, the tearing mode grows and saturates

•Initial equilibrium is unstable to several tearing modes; q=2 is the dominant instability.

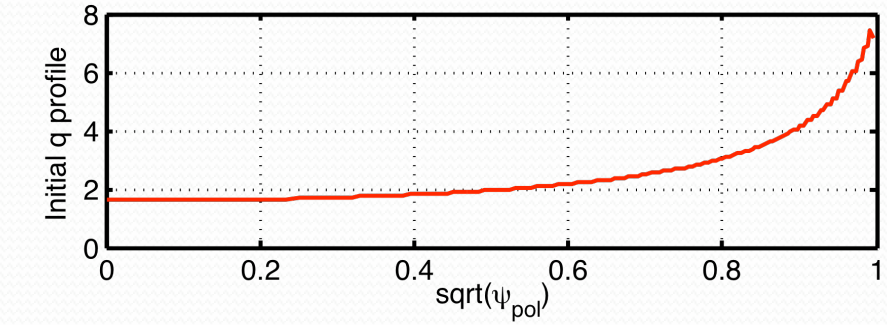

•The toroidal Fourier components of magnetic energy are associated with island structures; more energy implies greater island widths.

•Saturated island structure dominated by (2,1) mode

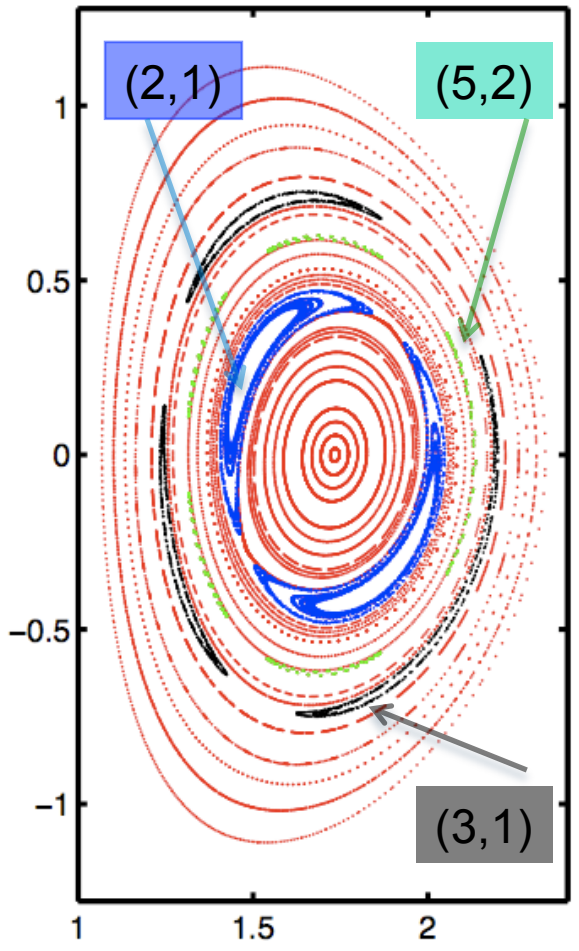

Alteration of the parallel current profile occurs at saturation

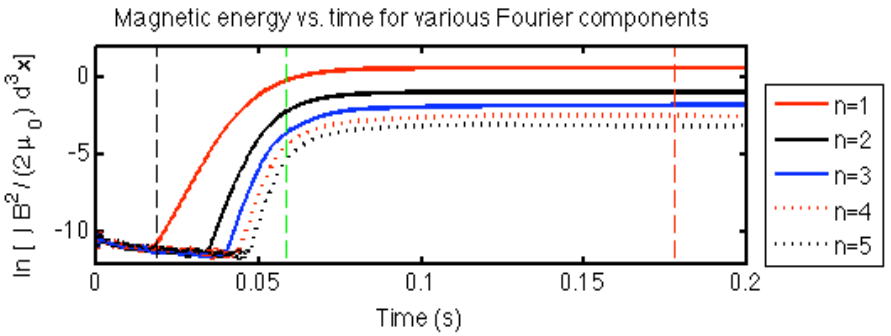

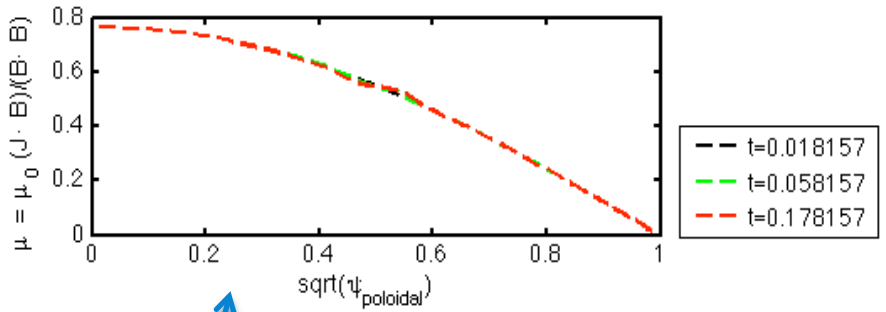

•Saturation has only minor effects on the q profile.

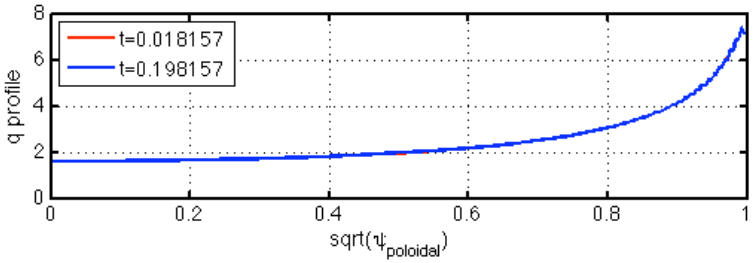

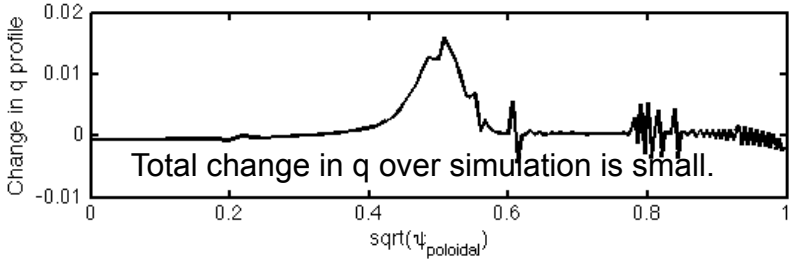

•Toroidally averaged μ profile (<μ>) and closeup. Relaxes to a quasilinearly flattened equilibrium at long times.

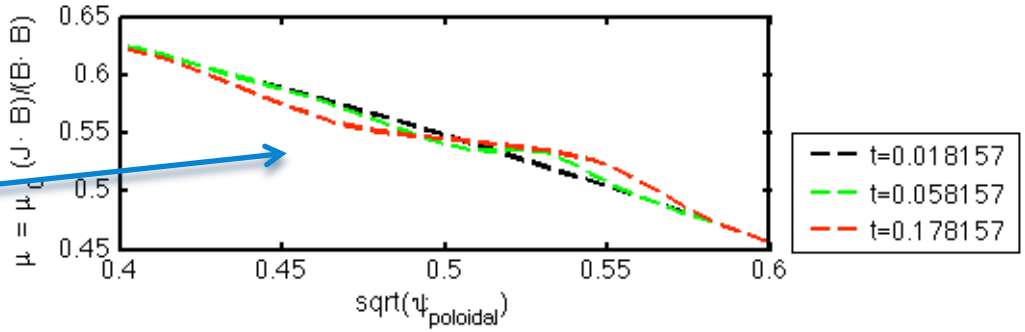

•A net flattening of <μ> near the rational surface is stabilizing (decreased <μ> inside, increased <μ> outside). Here, helical current perturbations are the cause of saturation.

Now, apply localized ECCD near the rational surface

•ECCD term: $$\frac{\mathbf{F}_{e0}^{rf}}{n|q_e|} = -\frac{\eta\lambda\mathbf{B}}{\mu_0} f(\mathbf{x})g(t)$$

•Choose $$f(\mathbf{x}) = \exp\left(-\frac{(R-R_{rf})^2 + (Z-Z_{rf})^2}{w_{rf}^2}\right)$$

(ignoring toroidal variation – ECCD is symmetric in ζ)

and

$$g(t) = \frac{1}{2}\left[\tanh\left(\frac{t-t_o}{t_p}\right) + \tanh\left(\frac{t_o}{t_p}\right)\right]$$

(ramping up after an offset t_o on a timescale t_p which is faster than the resistive time τ_R but slower than the Alfvén time τ_A).

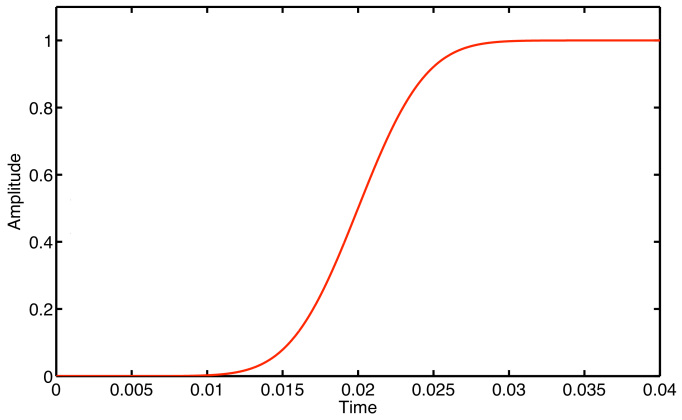

Complete suppression of the (2,1) resistive tearing mode has been achieved by the model

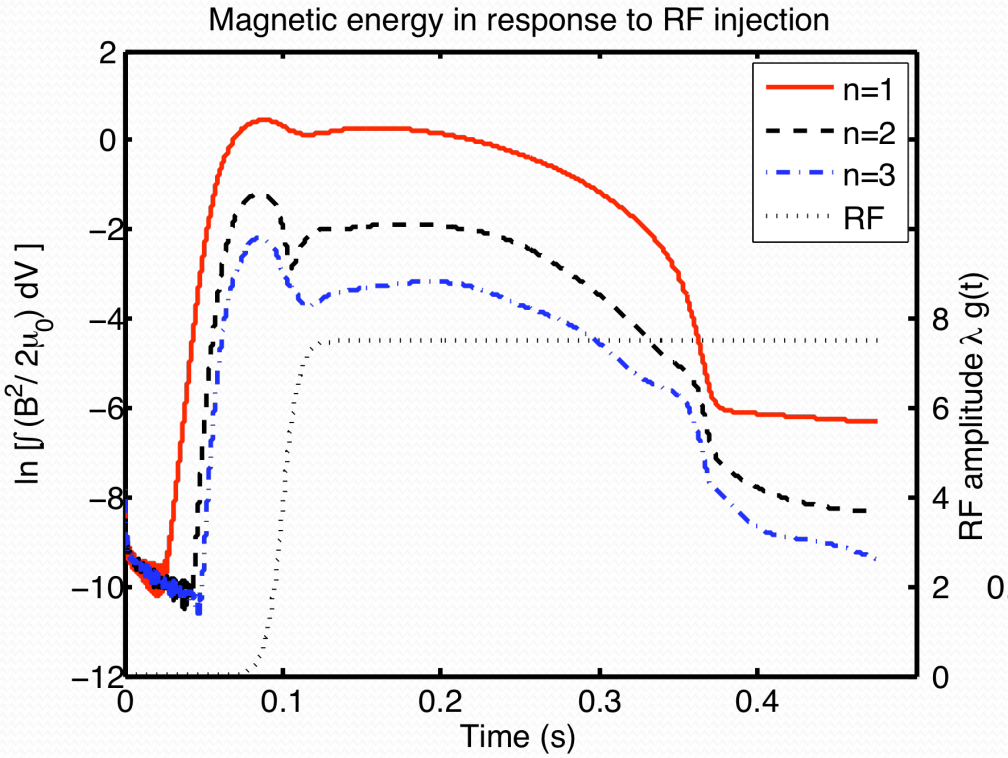

•Here, the RF (at long times) induces a net toroidal current whose value is ~3% of the initial toroidal current. This current ratio is determined by λ and the initial equilibrium.

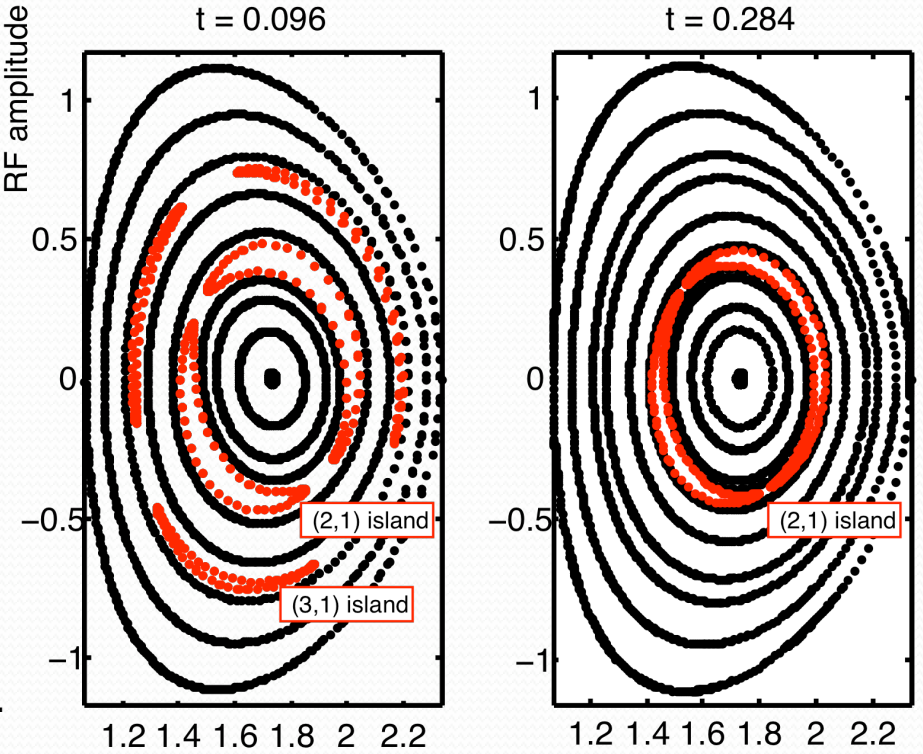

•Driven current is induced on a timescale ~ τ_R*(geometric factor related to poloidal ECCD localization). Here, τ_R = 0.064.

•By t=0.35, island structures have vanished.

What is the physics of the ECCD interaction with tearing modes?

- Tearing mode is influenced by toroidally symmetric ECCD in two major ways:

- Modification of tearing parameter Δ' (at long times)
  - -Altering Δ' affects linear growth rate, saturated island width

  - -Easy to diagnose and simulate – Δ' proportional to linear growth rate

- Alteration of "helical" current profile $\mu = \mu_0 (J \cdot B)/(B \cdot B)$ (at short times)
  - -Becomes important as mode saturates nonlinearly – more significant for existing islands. May interfere with or reinforce helical mode structures.

  - -Carries all effects of Δ'_{ECCD} in Rutherford equation.

  - -Harder to diagnose quantitatively.

Consider Δ' modification (an n=0 effect)

•We want to find the effect of n=0 ECCD perturbations, so temporarily turn off the other Fourier components in the MHD equations. (ECCD remains symmetric in ζ throughout simulation.)

•ECCD comes to steady state, eventually inducing a steady-state toroidal current. Takes a long time to reach steady state (geometric factors * τ_R, again)…

•Then turn on n>0 Fourier components and observe (2,1) tearing mode growth.

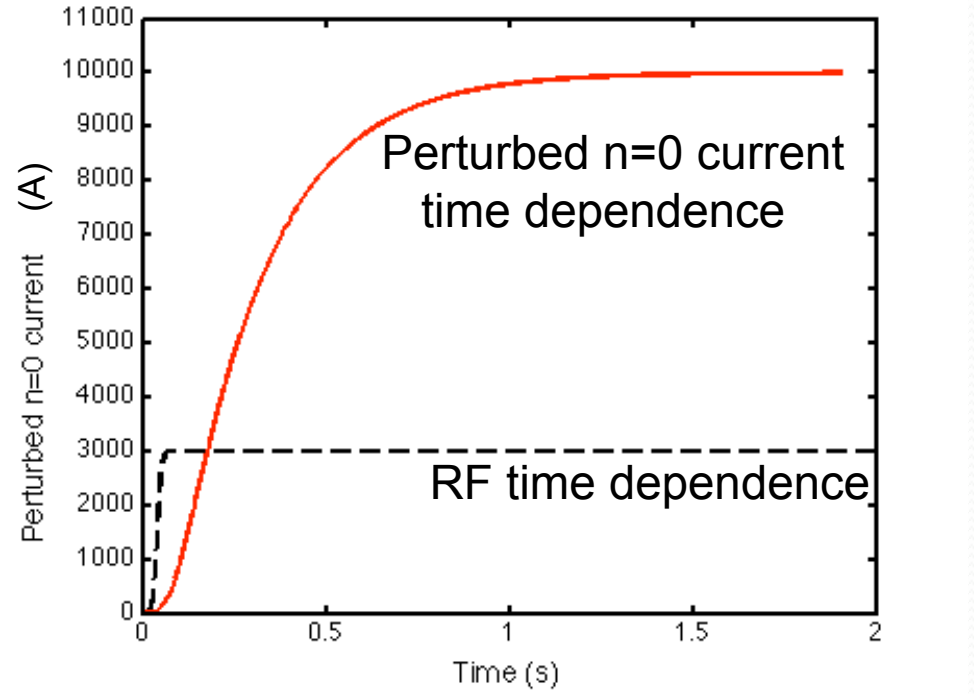

The rational surface position shifts in response to the ECCD

•Localize ECCD deposition to the outboard midplane (Z_{RF}=0) and center a fixed-width peak (w_{RF}=0.037) at various radial coordinates R_{RF}.

•The rational surface shifts outward, when deposition is centered inboard from (or even slightly outboard from) its original intersection with the midplane. Shift is larger for higher ECCD power (λ).

•This will have implications for the effectiveness of RF injection at high powers.

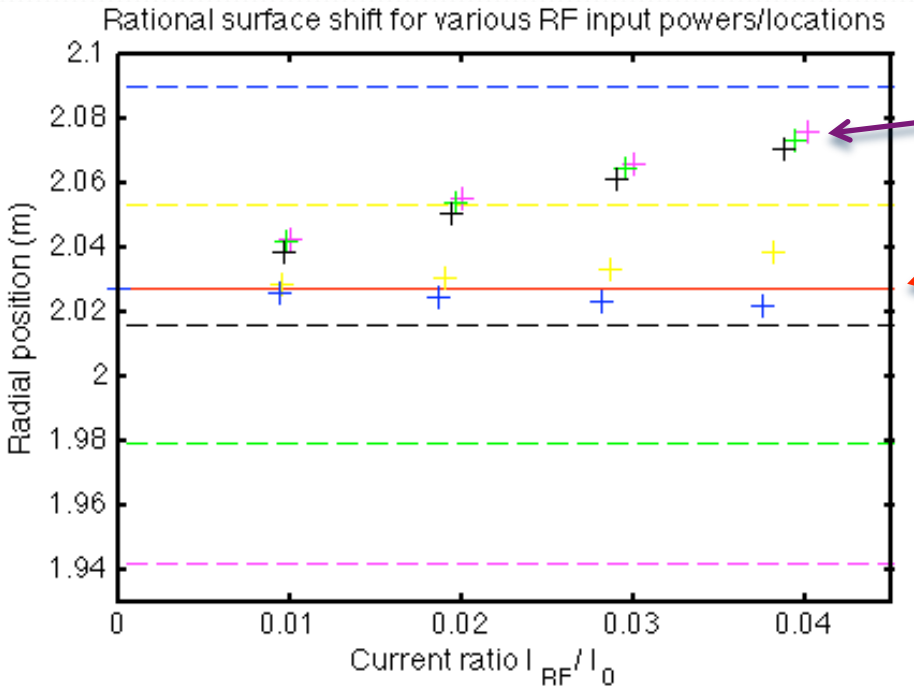

Shifted radial coordinate of rational surface on outboard midplane

Radial coordinate of original rational surface on outboard midplane

Radial coordinate of deposition peak, on outboard midplane

Width scale of Gaussian deposition

ECCD must be well aligned to favorably affect the growth rate

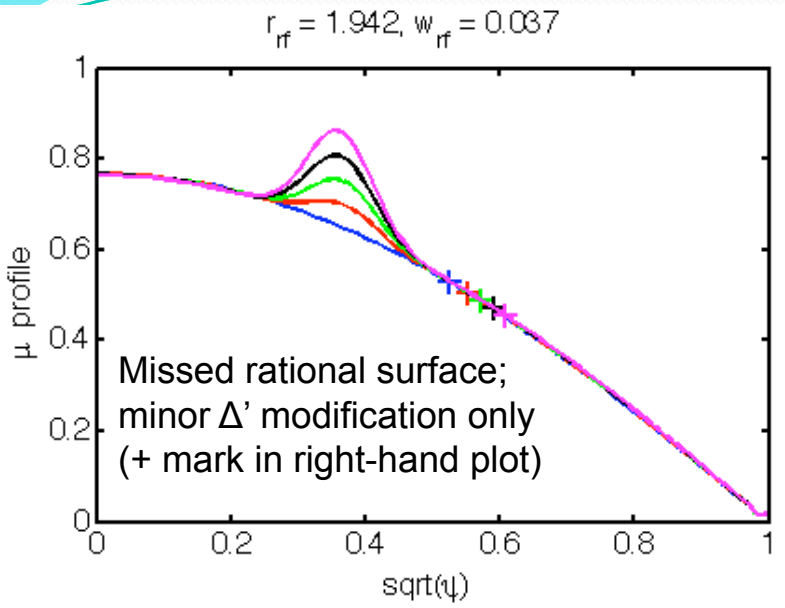

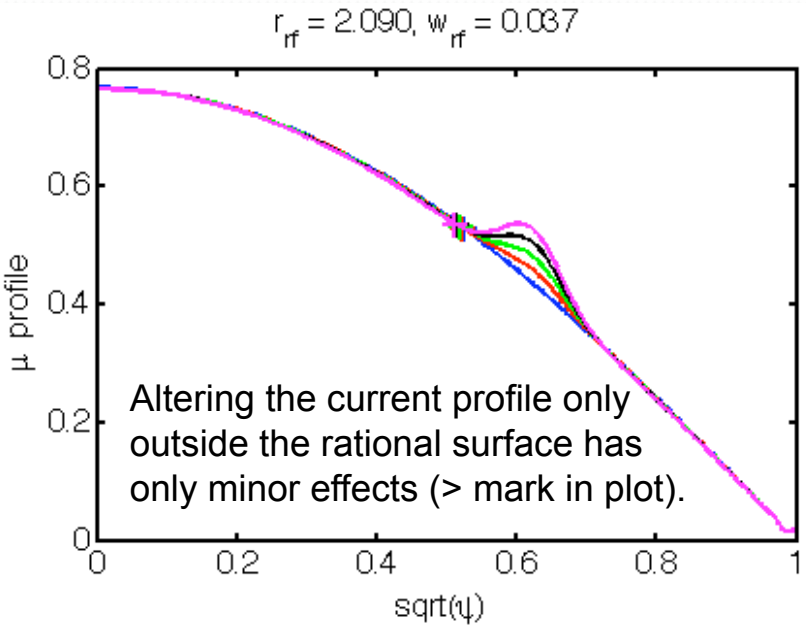

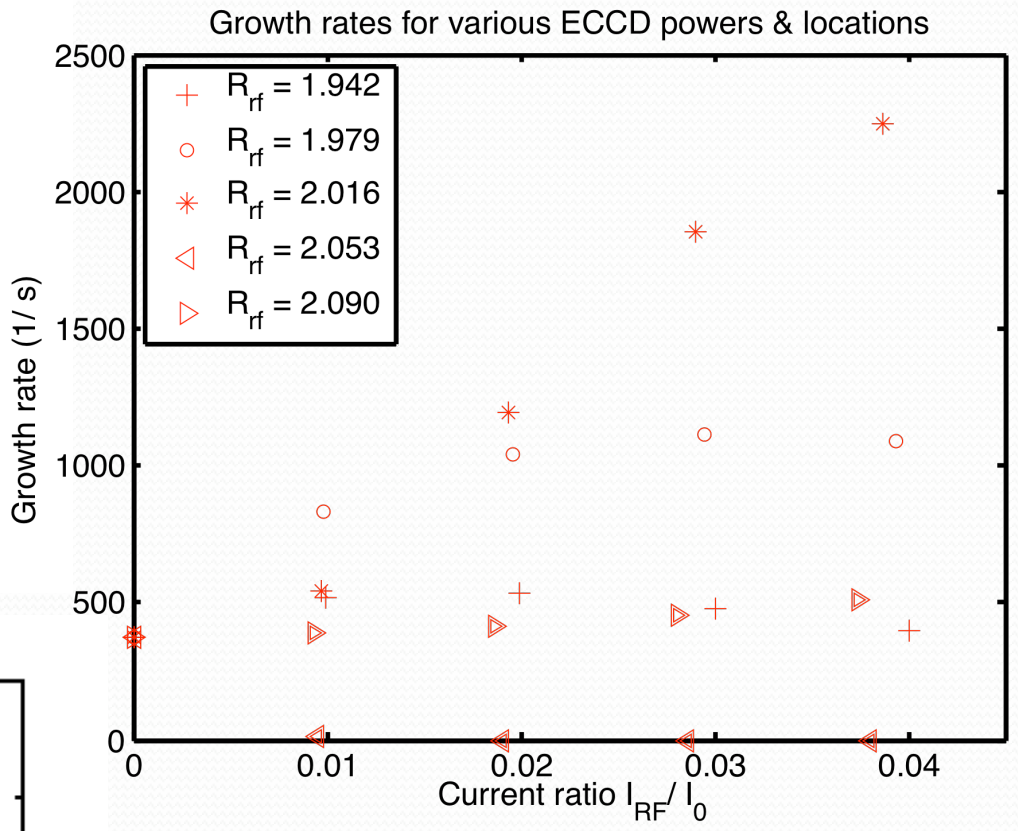

- Recall – a net flattening of <μ> around the rational surface should be stabilizing.

Here we have missed the rational surface altogether, so we don't expect to see large effects on the mode growth.

Misaligned ECCD may be affected by rational surface shifts

•Although higher ECCD input powers increasingly steepen <μ> profile near the original rational surface position, the increasing ECCD power also shifts the rational surface away from the deposition region.

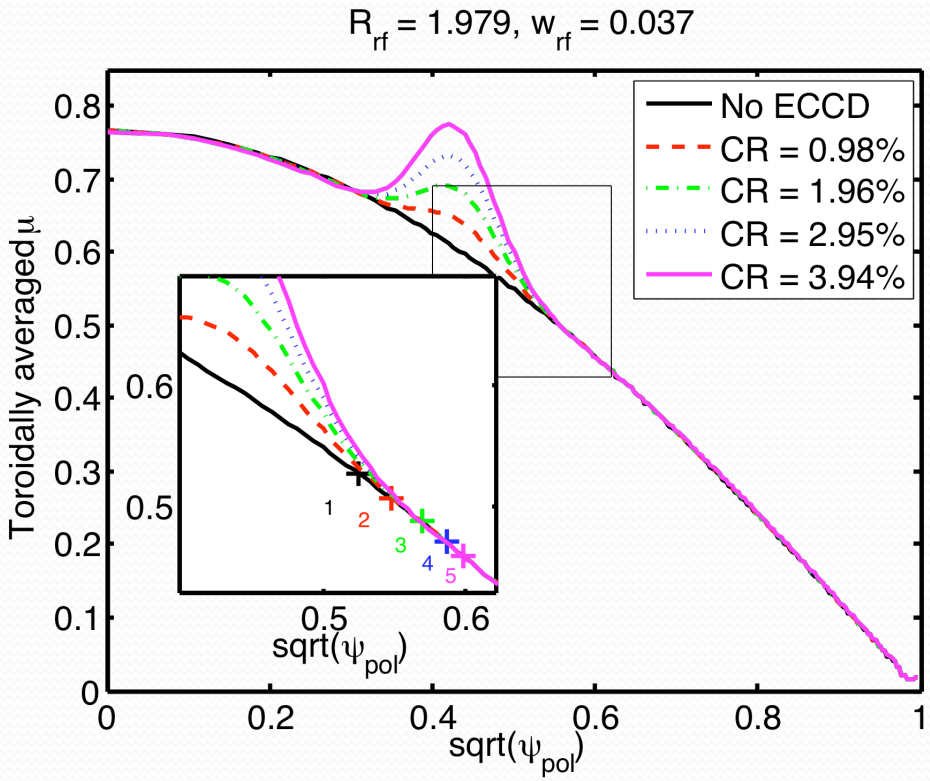

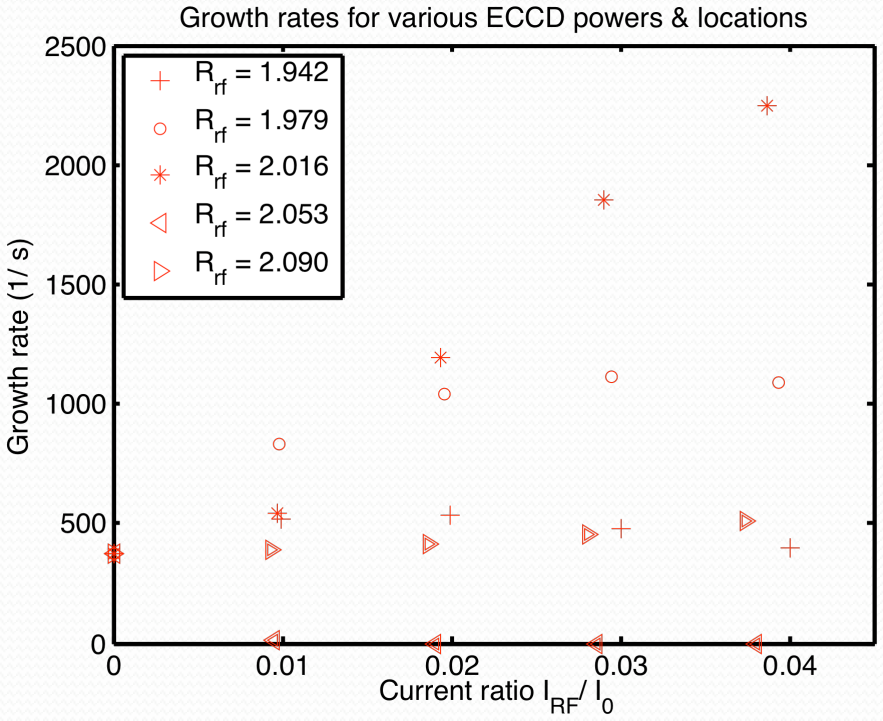

•The o marks in the above plot show the result; the growth rate is initially increased, but additional ECCD power doesn't alter it appreciably.

Misaligned ECCD can adversely affect the mode growth

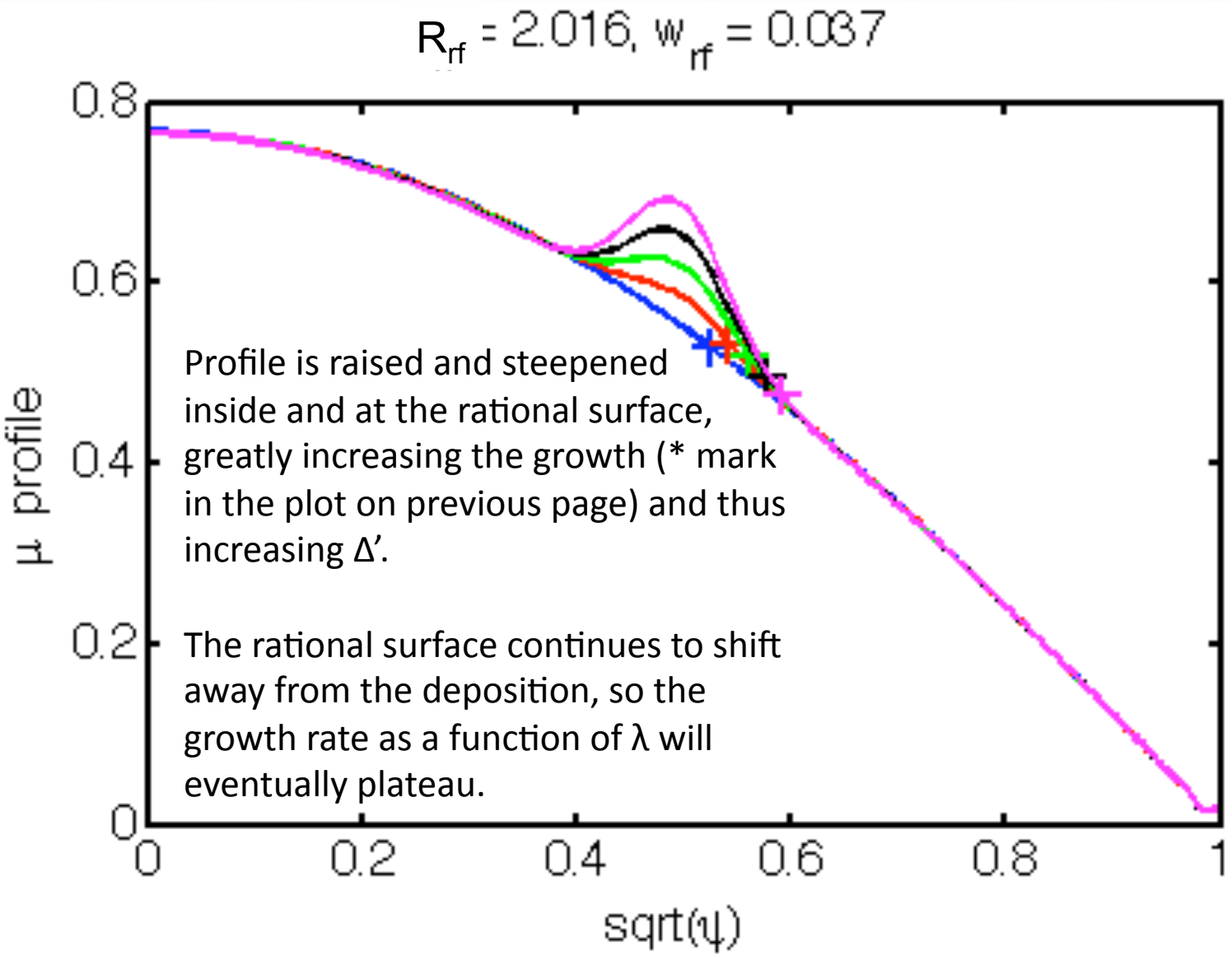

Profile is raised and steepened inside and at the rational surface, greatly increasing the growth (* mark in the plot on previous page) and thus increasing Δ'.

The rational surface continues to shift away from the deposition, so the growth rate as a function of λ will eventually plateau.

Proper ECCD alignment reduces the growth rate and may suppress the modes altogether

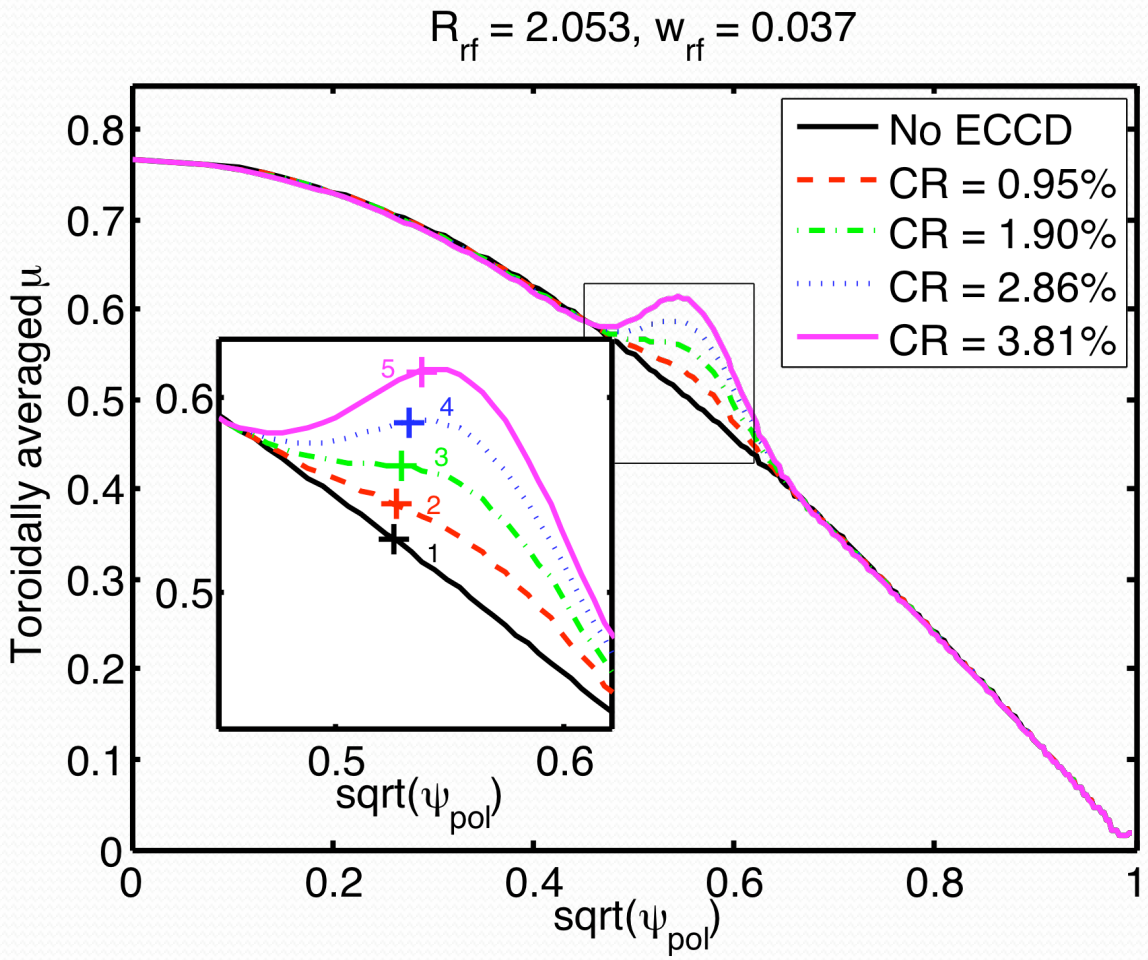

- ECCD deposition centered just outside the rational surface completely stabilizes the (2,1) mode for current ratios ≥ 2%. (See < marks in growth rate plot.)

- The movement of the rational surface across the deposition peak as the current ratio is increased will eventually destabilize this equilibrium.

Published results from the PEST-3 code can be explained in terms of the rational surface shift

- ✔ Deposition just inside rational surface is destabilizing
- ✔ Deposition just outside the rational surface is stabilizing
- ✔ Deposition on the rational surface is stabilizing only at low RF powers

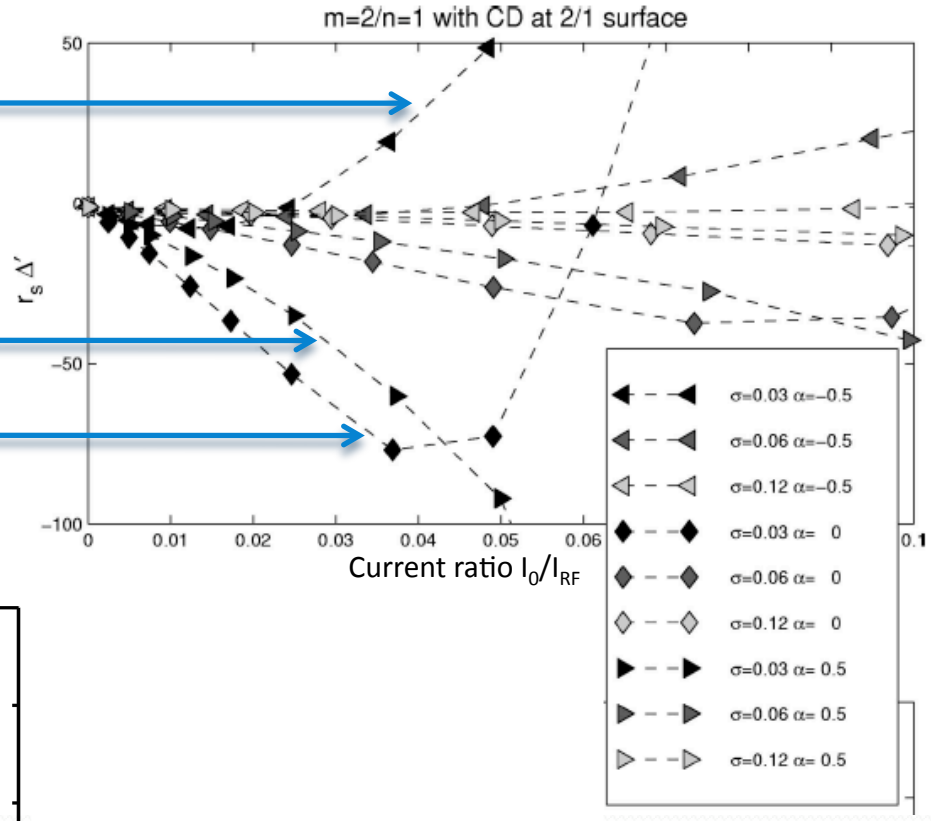

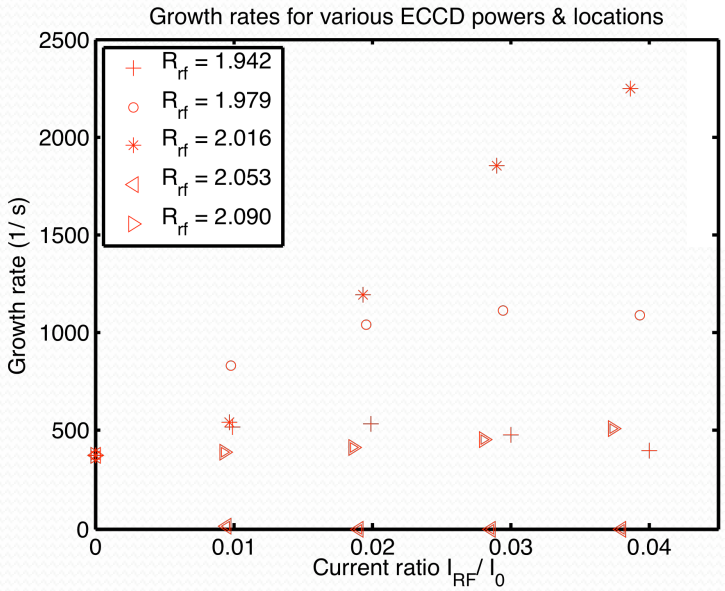

•Figure from Pletzer & Perkins, Phys. Plasmas **6**, 1589 (1999).

Tighter ECCD localization in the poloidal plane gives greater stability at the rational surface

- Agrees with Pletzer & Perkins result, as well as general conclusions of Hegna & Callen [Phys. Plasmas **4**, 2940 (1997)].

- Fairly weak RF drive here (current ratio 0.005), but trend should still hold.

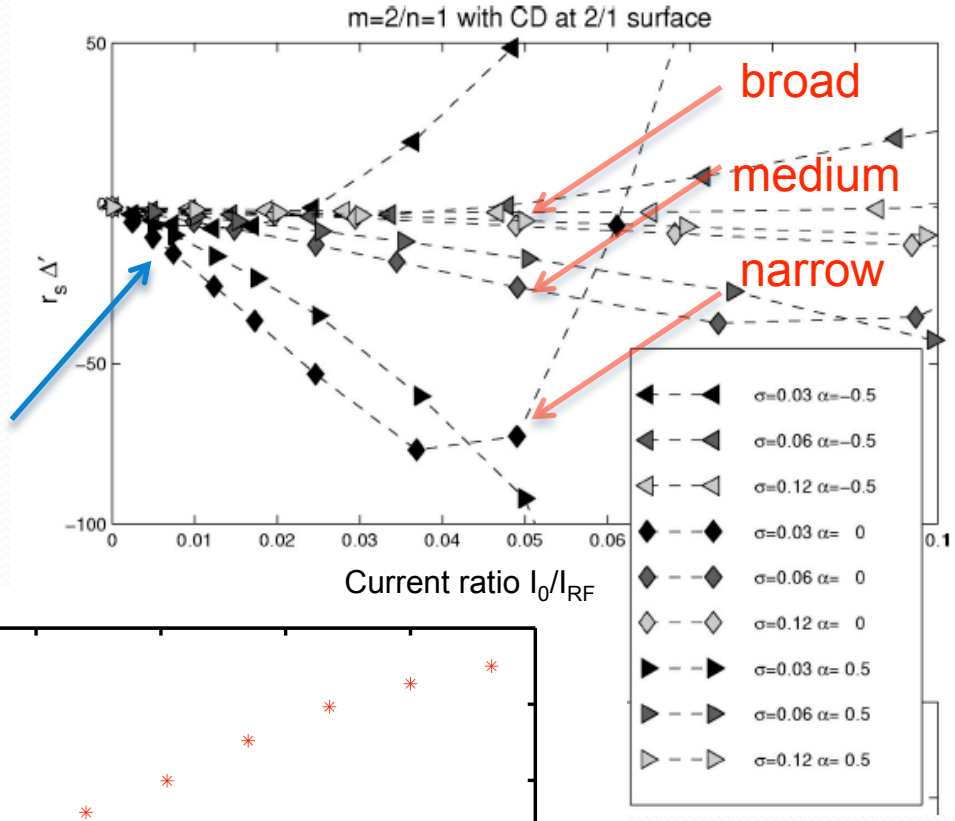

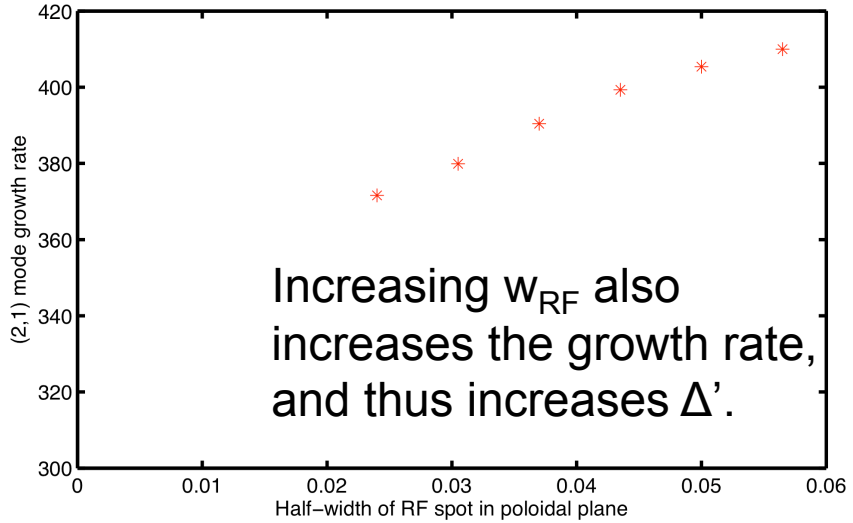

Now consider the effects of Δ'_{ECCD}

- The modified Ohm's law,

$$\mathbf{E} + \mathbf{u} \times \mathbf{B} = \eta \mathbf{J} - \frac{\eta \lambda \mathbf{B}}{\mu_0} f(\mathbf{x}) g(t)$$

has a component which can be written as

$$\frac{E_{\parallel}}{B} = \frac{\eta}{\mu_0} [\mu - \lambda f(\mathbf{x}) g(t)]$$

wherein the ECCD is balanced by parallel fields and currents.

- Analytic models (cylindrical geometry) suggest that the initial response to ECCD deposition is the creation of parallel electric field and the launch of Alfvén waves.

- Average the parallel Ohm's law over the flux surface – the ECCD component appearing in this equation, at long times, induces current while the corresponding parallel electric fields die away.

- Fluctuations of the ECCD about this average are countered by spatially fluctuating electric fields at long times; at short times, current fluctuations are also present. These fluctuations can adversely affect the mode growth rate if ECCD is poorly localized.

Δ'_{ECCD} effects can significantly increase mode growth when ECCD is misaligned

Dominated by Δ'_{ECCD} effects

Dominated by Δ' effects

	I_{RF}/I_0	R_{rf}	γ_1	γ_2	γ_{20}
	0.0000	—	371.88	371.88	371.88
misaligned	0.0100	1.942	683.89	660.31	518.49
	0.0200	1.942	888.35	781.23	539.39
	0.0300	1.942	1021.72	800.50	480.94
	0.0400	1.942	1135.77	799.41	397.78
	0.0098	1.979	1100.91	1094.48	834.50
	0.0196	1.979	1754.99	1659.61	1039.10
	0.0295	1.979	2334.12	2061.38	1113.18
	0.0394	1.979	2868.37	2350.39	1088.91
	0.0097	2.016	390.29	465.04	543.45
	0.0193	2.016	809.85	1089.22	1197.43
	0.0290	2.016	1689.10	2207.50	1854.23
	0.0387	2.016	2919.87	3516.81	2250.62
aligned	0.0095	2.053	104.18	86.03	13.39
	0.0190	2.053	29.32	0.00	0.00
	0.0286	2.053	187.45	79.15	0.00
	0.0381	2.053	522.13	524.81	0.00
misaligned	0.0094	2.090	453.34	448.92	389.69
	0.0187	2.090	494.42	485.79	417.78
	0.0281	2.090	546.98	515.96	452.30
	0.0374	2.090	593.47	560.39	509.67

- Use the same method as for Δ' modification – initially evolve only n=0 Fourier components of MHD equations, while ramping up toroidally symmetric ECCD.
- Instead of waiting for long-time effects associated with Δ' (i.e. the induced current coming to equilibrium at around twenty resistive times), turn on higher-order Fourier modes after only one or two resistive times have passed.
- The dominant influence on the growth rate will then come from short-time Δ'_{ECCD} effects.
- Growth rate is always increased at short times by misaligned ECCD.
- At high powers, even correctly aligned ECCD increases the growth rate (due to rational surface shift).

Characteristic Δ'_{ECCD} effects can be identified when the ECCD is misaligned

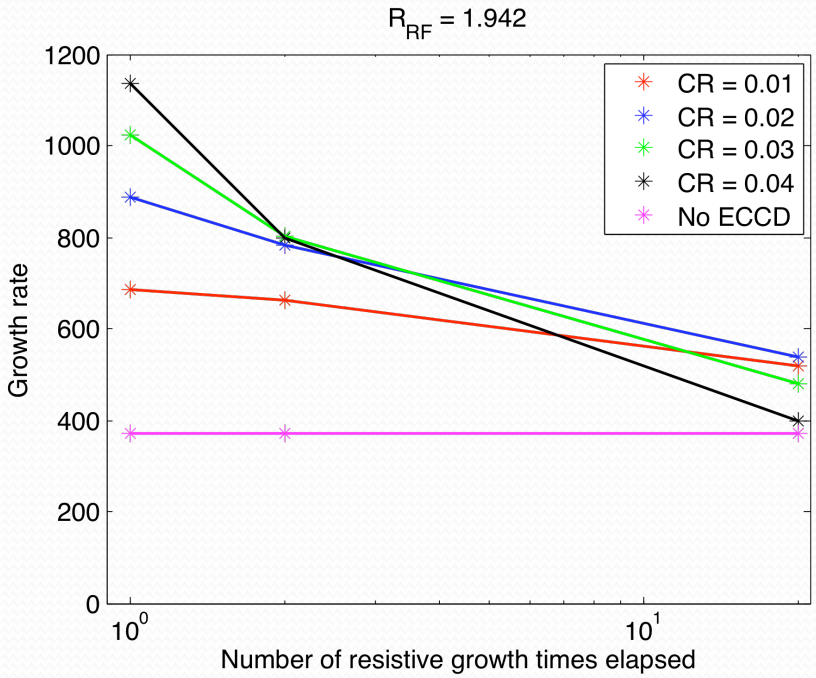

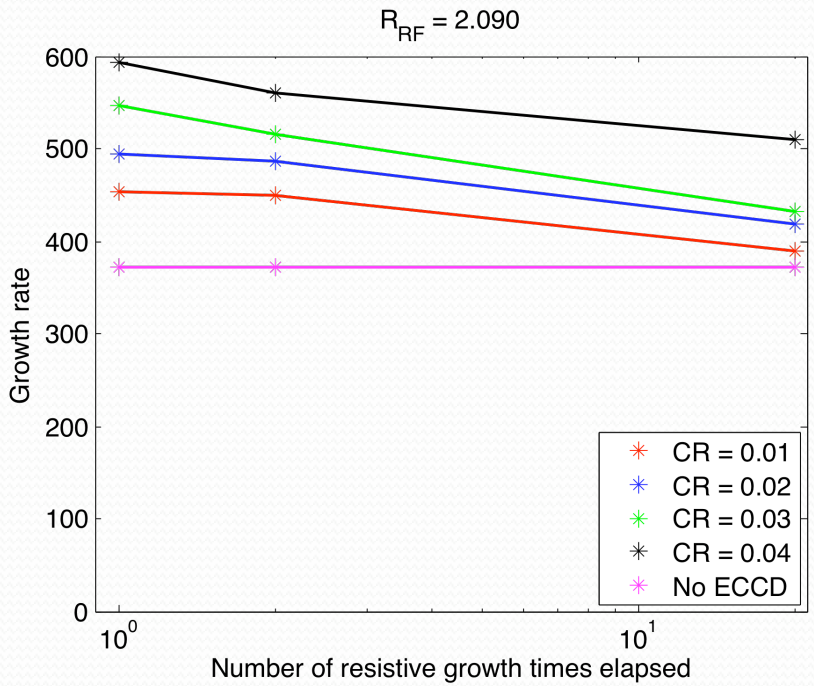

- Large ECCD misalignment initially raises the mode growth rate (relative to the rate occurring when ECCD is absent). The growth rates decrease as time passes, but are still elevated relative to the rate in the absence of ECCD.

Δ'_{ECCD} effects can indicate when proper spatial ECCD localization has been achieved

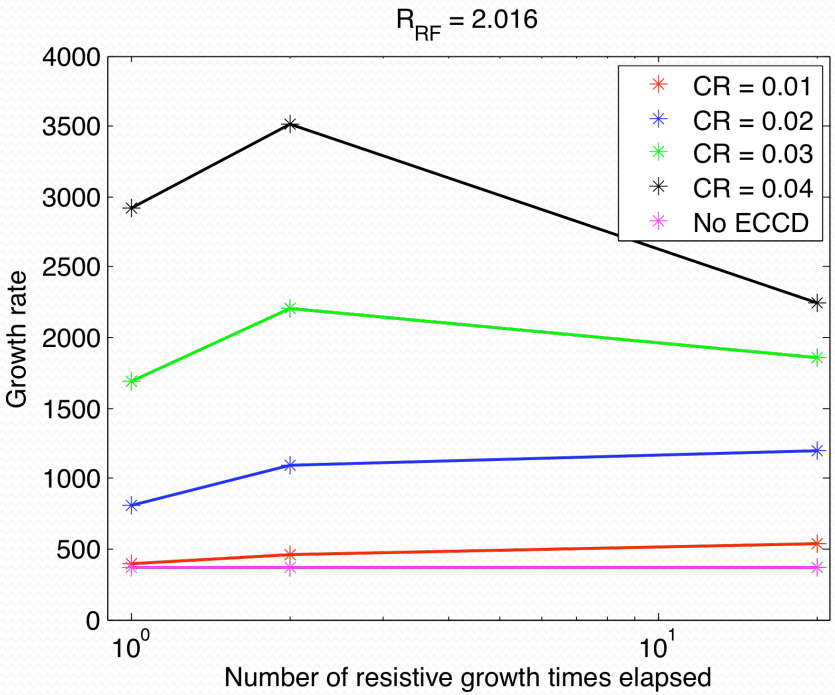

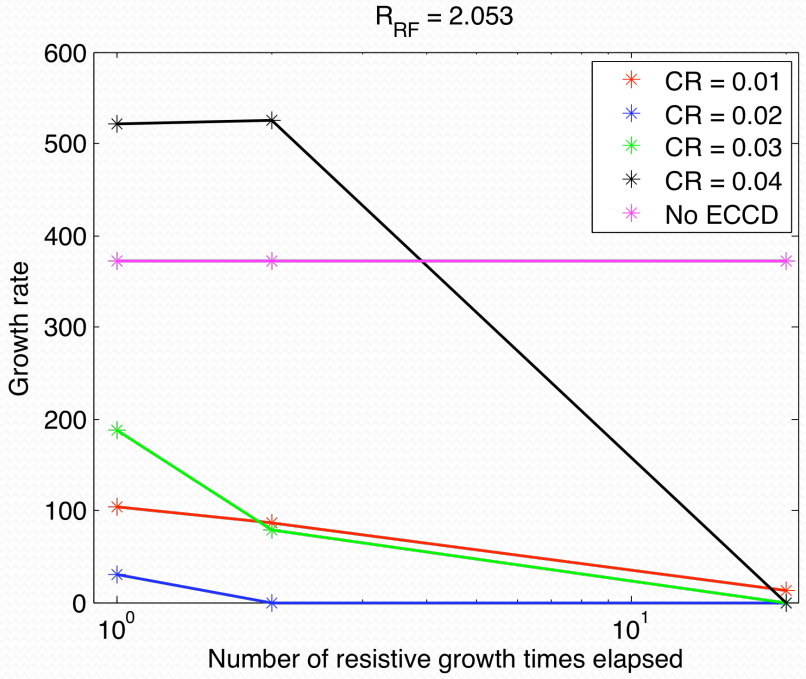

- ECCD deposition in the destabilizing region initially yields growth rates which are extremely high (relative to the case without ECCD) and which increase in time.

- Low-power (CR ≤ 3%) ECCD deposition in the stabilizing region yields lower growth rates which decrease in time.

For greater self-consistency, our model for ECCD can be replaced by GENRAY/CQL3D output

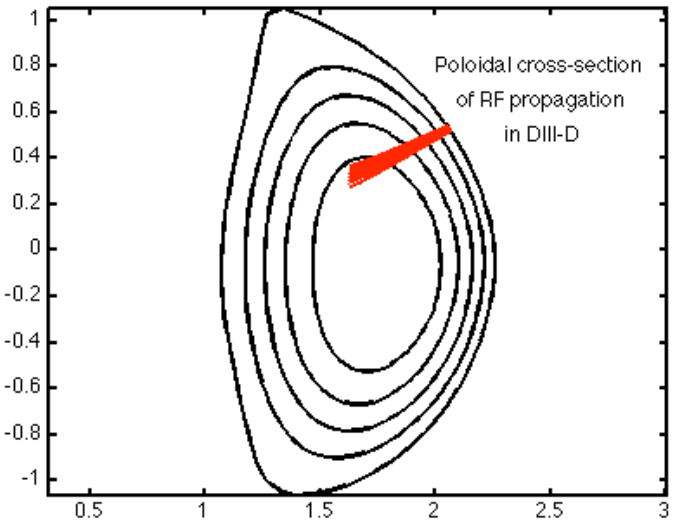

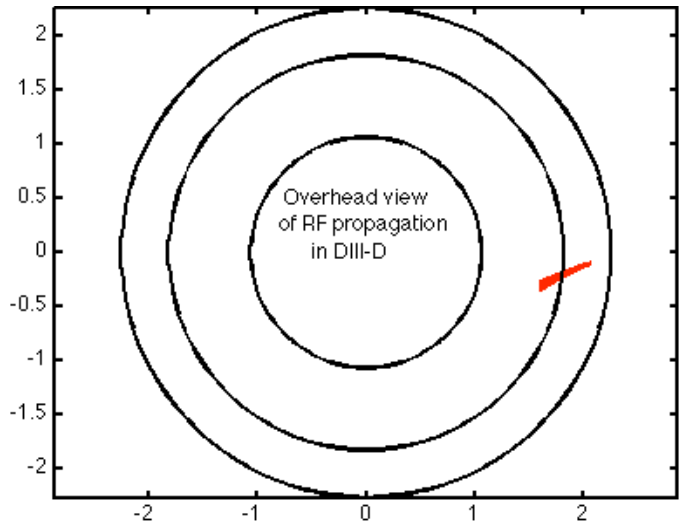

- NIMROD has been modified so that its magnetic geometry can be exported to GENRAY/CQL3D. ECCD ray trajectories, as well as localized current and power deposition, can then be calculated and returned to NIMROD.

- Ultimately, the full 5-D quasilinear operator will be passed from GENRAY to NIMROD.

- Methods to transfer discrete ray data to NIMROD's finite element basis functions are under development.

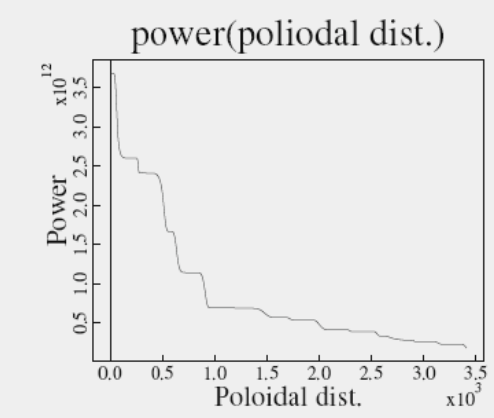

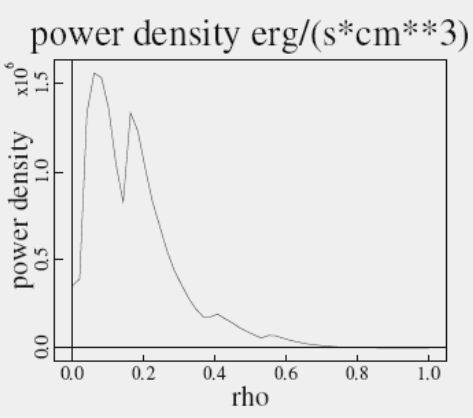

Ultimately, the NIMROD/GENRAY coupled system will be controlled by the Integrated Plasma Simulator (IPS)

•What the IPS does:

-Manages the interaction between multiple, coupled, multiprocessor physics components (e.g. individual codes such as NIMROD or GENRAY). Allocates processors for and initiates runs for various components when needed; manages data transfer between components.

-Organizes the data storage associated with the individual component codes, maintains "snapshot" of plasma as simulation progresses (Plasma State).

-Tracks provenance of data – how the various component codes used in the simulation were compiled, which code versions were used, which user set up and ran the simulation, etc.

-Provides monitoring capability for observing running and completed simulations.

•More information on IPS is available at http://cswim.org/ips

Schematic NIMROD/GENRAY coupling under IPS

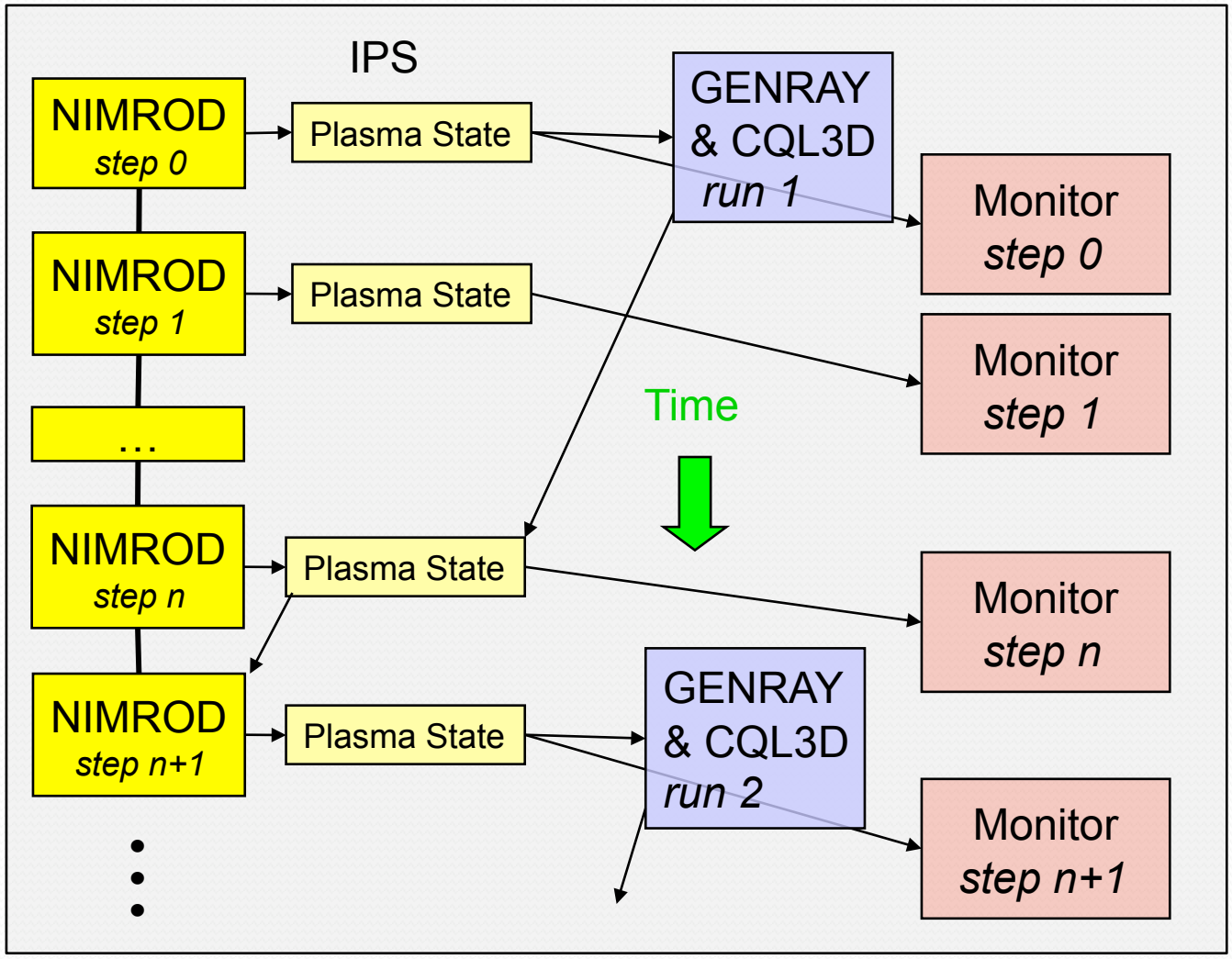

Data transfer handled by IPS through Plasma State (black arrows)

- Island geometry only weakly modifies magnitude of magnetic field
- Resonance condition of GENRAY changes weakly
- If greater sensitivity discovered, can move to tighter coupling

Upcoming developments

- GENRAY/CQL3D is coupled to IPS; NIMROD-IPS coupling not completed yet
- Passing of 5-D quasilinear operator from GENRAY to NIMROD
- Calculation of neoclassical closures for NTM studies – getting a self-consistent set of MHD equations with collisional, toroidal, and ECCD effects (with J. Ramos, MIT)
- Further testing of discrete-to-continuum interpolation methods – getting discrete GENRAY data onto NIMROD's finite element basis functions
- Efficiency of time-modulated ECCD for rapidly rotating equilibria